# Copper(I) and Copper(II) Uranyl Heterometallic Hybrid Materials

Zhehui Weng,[†] Zhi-hui Zhang,[†] Travis Olds,[†] Marcin Sterniczuk,[‡] and Peter C. Burns*[†,‡]

[†]Department of Civil and Environmental Engineering and Earth Sciences and [‡]Department of Chemistry and Biochemistry, University of Notre Dame, Notre Dame, Indiana 46556, United States

Ⓢ *Supporting Information*

ABSTRACT: Two copper−uranium heterometallic compounds, $[(UO_2)_3Cu^{II}O_2(C_6NO_2)_5]$ (**1**) and $[(UO_2)Cu^{I}(C_6NO_2)_3]$ (**2**), have been synthesized by the reaction of uranyl acetate with copper salts in the presence of isonicotinic acid. Both compounds have been characterized by single-crystal X-ray diffraction, IR, Raman, and UV−vis spectroscopy. In compound **1**, interactions between copper and uranium centers occur and result in a three-dimensional pillar layered structure. Compound **1** is also the first example of a heterometallic uranyl organic framework with a trinuclear U_3O_{18} building block. Compound **2** is the first uranyl organic framework that contains monovalent copper, which arises from the reaction of Cu(II) chloride and is assumed to be due to the oxidation of chloride at low pH.
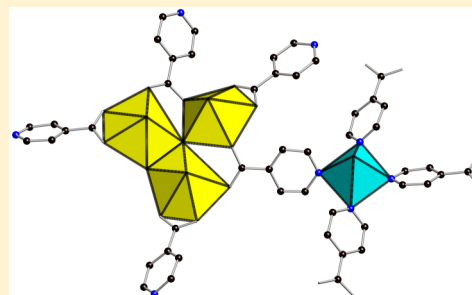
INTRODUCTION

The design and synthesis of uranyl−organic coordination polymers or frameworks (UOFs) presents intriguing structures, as well as compounds with interesting physicochemical properties and potential value in the nuclear fuel cycle.[1−5] The coordination chemistry of U(VI) is heavily dominated by the linear $(UO_2)^{2+}$ uranyl ion. This moiety occurs coordinated by four, five, or six coplanar (or nearly so) ligands, giving square, pentagonal, and hexagonal bipyramids with the O atoms of the uranyl ions located at the polyhedral apicies.[6,7] Structural sheets commonly result from the linkage of uranyl bipyramids through the sharing of equatorial vertices or edges with other uranyl polyhedra or other cation-centered polyhedra. The uranyl ion contains triple U≡O bonds,[8] and as a result, its O atoms are often terminal in the structural unit. Thus, the most common structural theme in uranyl compounds is the presence of complex sheets of uranyl and other polyhedra that form an anionic structural unit, with low-valence cations and often H_2O in the interstitial (interlayer) complex.

Synthetic approaches that favor formation of UOFs are of interest, with the primary goal of providing linkages between structural units that are compatible with the bond strengths within the uranyl ion. A proven strategy for the synthesis of UOFs is to associate metallic centers with O- or N-donor organic ligands, which can result in the formation of multidimensional coordination polymers.[9] Many N-bearing and carboxylate-based organic ligands have been used to yield UOFs.[1,10,11] Using derivatives of either pyridinecarboxylate and/or benzoic acid, several organic uranyl polymers have been synthesized and characterized. These consist of either single-vertex or edge-sharing uranyl pentagonal bipyramids that are connected by organic ligands, resulting in a series of mononuclear oligomers, ribbon-like chains, sheets, and extended frameworks.[12−15]

An alternative strategy for assembling UOFs is to introduce other distinct heterometallic elements, such as lanthanides or transition metals, into the uranyl structural unit.[9] Several 3d−5f heterometallic UOFs have been synthesized, the majority of which are constructed with inorganic coligands including sulfate, arsenate, phosphate, and others ligands.[16−24] As such, 3d metals are good candidates for this purpose.

Copper is well known for the Jahn−Teller effect associated with Cu(II) in octahedral coordination and valence state flexibility. The Jahn−Teller effect is usually manifested as octahedra with four short Cu−ligand bonds in a square planar arrangement and two longer axial Cu−ligand bonds, resulting in an elongated (4+2) octahedral geometry.[9,25] Cu(I) cations usually have unique electron-transfer behavior and are important in many biological processes.[26−29] Relatively few Cu−U heterometallic compounds have been reported, and most that have exhibit UOFs with divalent copper.[9,17,21,30−41] We are unaware of UOFs containing Cu(I) in the literature.

We are interested in assembling copper−uranium compounds by using isonicotinic acid as a ligand source, with the intent that both the organic species and the 3d metal may increase functionality of the resulting compounds. Also of interest are the variable copper oxidation states that may result from this synthetic route. Two phases with different oxidation states of copper, $[(UO_2)_3Cu^{II}O_2(C_6NO_2)_5]$ (**1**) and $[(UO_2)Cu^{I}(C_6NO_2)_3]$ (**2**), have been synthesized and isolated. Herein, we report the synthesis, crystal structures, and characterization of these new compounds. The $U^{VI}≡O−Cu^{II}$ interaction in compound **1** is a relatively unusual configuration[20,34,42−49] that is similar to that found in a recent report by Arnold and Loiseau.[50,51]

EXPERIMENTAL SECTION

Synthesis. *Caution! Although depleted uranium was used in these studies, standard precautions for handling radioactive materials should be followed.*

$[(UO_2)_3Cu^{II}O_2(C_6NO_2)_5]$ (**1**) and $[(UO_2)Cu^I(C_6NO_2)_3]$ (**2**) were synthesized by reacting uranyl acetate with either Cu(II) acetate or Cu(II) chloride (Scheme 1). All chemicals were acquired from

Scheme 1. Synthesis of Compounds 1 and 2
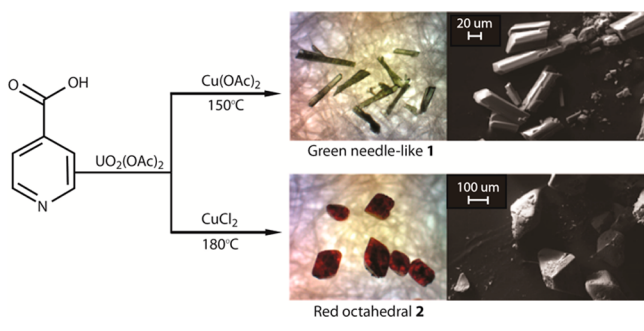
commercial suppliers and used without further purification. Distilled and Millipore filtered water with a resistance of 18.2 MΩ cm was used in all reactions. The temperature and starting copper(II) salts are very important in the formation of **1** and **2**. In the presence of Cl⁻, the Cu(II) cation is reduced to Cu(I) at 180 °C, whereas reduction is not observed in the analogous reaction at 150 °C.

$[(UO_2)_3Cu^{II}O_2(C_6NO_2)_5]$ (1). Uranyl acetate (0.058 mmol, 0.0248 g), Cu(II) acetate (0.5 M, 0.05 mL), isonicotinic acid (0.075 mmol, 0.0092 g), and 2 mL of water were heated at 150 °C in a 23 mL Teflon-lined stainless steel reaction vessel for 4 days, followed by cooling to room temperature at a rate of 0.1 °C min⁻¹. Green needle-like crystals of **1** (133 mg of product, in ca. 57.4% yield based on Cu) and blue sheet-like plates (known structure of copper di(isonicotinate) tetrahydrate, confirmed by X-ray diffraction) were collected by filtration of the reaction mixture followed by washing with distilled water. The initial and final pH values of this reaction were 3.33 and 3.46, respectively. Phase purity was confirmed by comparing simulated and observed powder X-ray diffraction patterns (Figure S1).

$[(UO_2)Cu^I(C_6NO_2)_3]$ (2). Uranyl acetate (saturated aqueous solution, 1.2 mL), Cu(II) chloride (0.5 M, 0.1 mL), isonicotinic acid (0.2 mmol, 0.0247 g), and 0.8 mL of water were heated at 180 °C in a 23 mL Teflon-lined stainless steel reaction vessel for 4 days, followed by cooling to room temperature at a rate of 0.1 °C min⁻¹. Dark red octahedral crystals of **2** (100 mg of product, in ca. 29.1% yield based on Cu) and a small amount of black powder were collected by filtration and were washed using distilled water. The initial and final pH values were 3.04 and 3.23, respectively. Comparison of the simulated and observed powder X-ray diffraction patterns demonstrated phase purity (Figure S2).

Single-Crystal X-ray Diffraction and Powder X-ray Diffraction. Suitable single crystals of **1** and **2** were selected under cross-polarized light. Each was mounted on a glass fiber for single-crystal X-ray diffraction studies using a Bruker APEX II Quazar diffractometer equipped with graphite-monochromated Mo Kα X-radiation provided by a microfocus source combined with Montel optics. A sphere of data was collected at room temperature for each compound using frame widths of 0.5° in ω. Data were integrated and corrected for background, Lorentz, and polarization effects using the APEX II software.[52] Data were corrected for absorption empirically using SADABS.[53] Each structure was solved and refined using SHELXTL[54] on the basis of F^2. Selected crystallographic parameters are provided in Table 1, and selected bond lengths and angles are in Tables 2 and S1. Full details of the structures are in the Supporting Information.

Powder X-ray diffraction patterns of **1** and **2** were collected using a Bruker θ−θ diffractometer equipped with a Lynxeye one-dimensional solid-state detector and Cu Kα radiation from 5° to 50° (2θ) with a

Table 1. Crystallographic Data and Structure Refinement Results for Compounds 1 and 2

	1	2
structure formula	$[(UO_2)_3Cu^{II}O_2(C_6NO_2)_5]$	$[(UO_2)Cu^I(C_6NO_2)_3]$
fw	1543.98	687.78
cryst syst	monoclinic	orthorhombic
space group	$P2/c$	$Aba2$
a (Å)	9.7137(11)	27.757(3)
b (Å)	14.5743(16)	10.7340(11)
c (Å)	14.5114(16)	14.1940(15)
β (deg)	105.0120(13)	90
V (Å^3)	1984.3(4)	4229.1(8)
Z	2	8
ρ_{calcd} (g/cm^3)	2.584	2.160
μ (mm^{-1})	12.821	8.703
R_{int}	0.0683	0.0730
R_1 $[I > 2\sigma(I)]$	0.0296	0.0459
wR_2 (all data)	0.0681	0.1142
GOF on F^2	1.027	1.045
$\Delta\rho_{max}$, $\Delta\rho_{min}$ (e Å^{-3})	1.14, −0.75	0.67, −0.73

step width of 0.05° and a fixed counting time of 1 s/step. Patterns were calculated from the crystallographic parameters using Mercury.[55]

Spectroscopic Measurements. Electon paramagnetic resonance (EPR) spectra for a powdered sample of complex **1** were recorded with an X-band (9.5 GHz) Bruker EMX Plus spectrometer at room temperature. The field modulation was in the range 1 to 5 G, the modulation frequency was 100 kHz, and the microwave power was 0.05 to 1 mW. Absorption and fluorescence data were acquired for crystals of **1** and **2** using a Craic Technologies UV−vis−NIR microspectrophotometer with a fluorescence attachment. Absorption data over the range 250−1500 nm were collected under ambient conditions. Infrared spectra were collected from powdered specimens of **1** and **2** using a SensIR Technology IlluminatIR FT-IR microspectrometer equipped with an attenuated total reflectance (ATR) objective. The spectra were taken from 600 to 4000 cm⁻¹ with a beam aperture of 100 μm for samples stored in a desiccator for 24 h prior to analysis. Raman spectra were collected under ambient conditions for single crystals of **1** and **2** using a Bruker Sentinel system linked by fiber optics to a Raman probe held in a microscope mount. The laser wavelength was 785 nm with a power of 400 mW. Energy dispersive spectra were collected for crystals of each compound using a LEO EVO 50 scanning electron microscope. X-ray photoelectron spectroscopy measurements were carried out with an XPS PHI VersaProbe II X-ray photoelectron spectrometer at room temperature. The C 1s peak of adventitious carbon at 284.6 eV was used for calibration.

RESULTS

Single-crystal X-ray analysis revealed that compound **1** contains two symmetrically distinct uranyl cations, one Cu(II) cation, and three isonicotinate anions. The isonicotinate anions adopt three distinct coordination modes by acting as terminal, bridging, and triconnected ligands, as illustrated in Figure 1a. The Cu1 center is six-coordinated with a typical (4+2) environment due to the Jahn−Teller effect arising from the electronic degeneracy of Cu(II) in a holosymmetric octahedral ligand field.[9,25] There are four pyridyl N atoms with pairs of Cu−N bond lengths at 2.034(5) and 2.037(6) Å and two uranyl oxo atoms with Cu−O distances of 2.480(5) Å. The bond-valence sum at Cu1 is 2.08 vu (valence units),[56] consistent with the expected valence and green color of Cu(II). Both U(VI) cations are present as typical uranyl ions with bond lengths ranging from 1.771(5) to 1.799(5) Å. The calculated bond-valence[57] sums at the uranyl ions are 5.8 and

Table 2. Selected Bond Lengths (Å) for Compounds 1 and 2

compound 1				compound 2	
U1−O1	2.259(3)	U2−O9	2.445(5)	U1−O1	2.508(9)
U1−O2	1.799(5)	U2−O9[a]	2.444(5)	U1−O2	2.451(8)
U1−O3	1.776(5)	U2−O10	1.771(5)	U1−O3	2.318(9)
U1−O4	2.288(4)	U2−O10[a]	1.771(5)	U1−O4[f]	2.361(8)
U1−O5[c]	2.573(5)	Cu1−N1	2.037(6)	U1−O5	2.302(7)
U1−O6[c]	2.490(5)	Cu1−N2	2.034(5)	U1−O7	1.762(10)
U1−O7	2.471(5)	Cu1−N1[b]	2.037(6)	U1−O8	1.727(9)
U2−O1	2.247(6)	Cu1−N2[b]	2.034(5)	Cu1−N1	1.955(12)
U2−O8	2.354(5)	Cu1−O2[d]	2.480(4)	Cu1−N2	1.979(10)
U2−O8[a]	2.354(5)	Cu1−O2[e]	2.480(4)	Cu1−N3	2.112(10)
				Cu1−O6	2.274(12)

[a]1−x, +y, 1/2−z. [b]2−x, +y, 3/2−z. [c]+x, −1+y, +z. [d]+x, 1−y, z−1/2. [e]2−x, 1−y, 1−z. [f]−x, 2−y, +z.
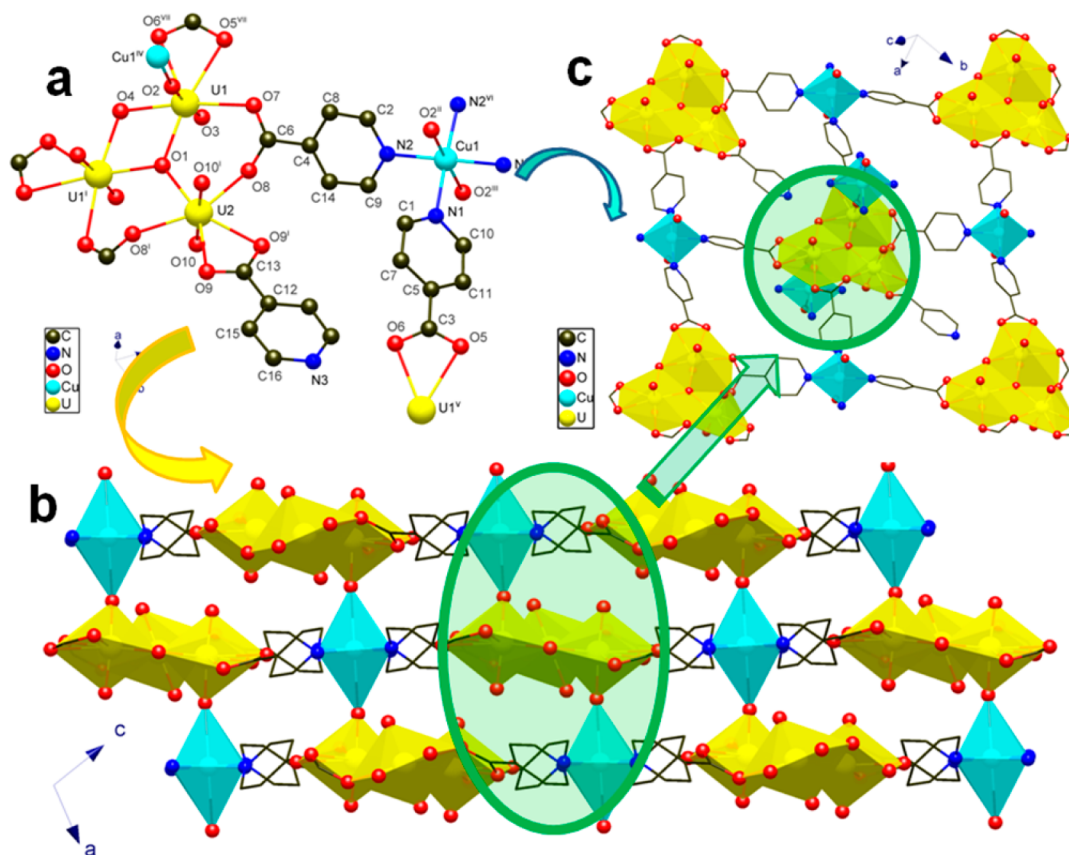

Figure 1. (a) Depiction of the coordination environments of the three U^{VI} sites and one Cu^{II} site in compound **1**. (b) Three-dimensional coordination structure indicating the heterometallic U≡O−Cu interactions. (c) Perspective of the three-dimensional network.

6.1 vu, respectively, consistent with the expected oxidation state. Both of the uranyl ions are equatorially coordinated by five oxygen atoms with bond lengths in the range 2.247(6) to 2.573(5) Å, similar to those reported for other pentagonally coordinated uranyls.[36] The two inequivalent crystallographic uranyl centers form a U$_3$O$_{18}$ trinuclear motif, built through the linkage of a μ^3-O1 atom, with additional bridging through the O4 atom. The trinuclear uranyl core is linked to two symmetry-related Cu(II) centers through a U≡O−Cu interaction. The resulting units are connected to each other through isonicotinate to construct a three-dimensional pillar layered structure (Figure 1b). The overall coordination structure of **1** consists of sheets formed by trinuclear U(VI) clusters with a U≡O−Cu interaction linking them (Figure 1c).

The U≡O−Cu interaction in **1** is somewhat unusual because of the strength of the U≡O bonding within the uranyl ion. However, the Jahn−Teller distortion of the Cu(II) octahedron results in a relatively low Cu−O bond strength, which facilitates the interaction. Several recent publications have designated interactions between uranyl ions and transition metal cations as cation−cation interactions (CCIs).[9,20,34,50,51] Historically, in actinide chemistry a CCI involves the interaction of an O atom of an actinyl ion with a second actinyl ion, and it is only recently that the definition appears to have been expanded to include the bonding of a uranyl ion O atom to various other cations.[51] We prefer to conform to the earlier definition of CCI and therefore do not designate the U≡O−Cu interaction in **1** as such. However, it is important to
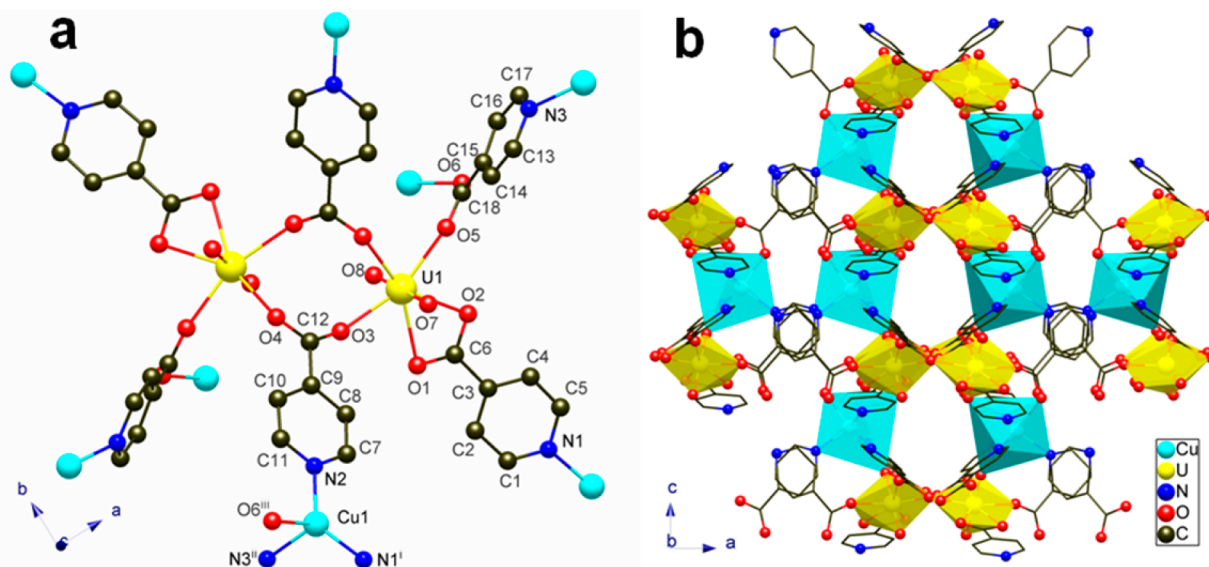
Figure 2. (a) Depiction of the coordination environments of the two U^{VI} sites and one Cu^{I} site in compound **2**. (b) Three-dimensional coordination structure showing the complicated network.

note that the interaction is analogous to those reported as CCIs for Cu(II),[9,34] Zn(II),[20] and Ln(III)[51] and that this interaction facilitates formation of a three-dimensional structure.

The asymmetric unit of **2** consists of one crystallographically unique uranyl cation, one Cu(I) cation, and three isonicotinate anions. The unusual terminal coordination mode with a free pyridyl N atom seen in **1** is absent here, with one isonicotinate anion being a bridging ligand and the other two serving as triconnected linkers. The Cu(I) center is four-coordinated by three pyridyl N atoms and one carboxylate O atom from four organic linkers. Two uranyl groups are joined by a pair of triconnected organic anions to form a binuclear cluster in which each U(VI) cation occurs in a pentagonal bipyramidal coordination geometry with five equatorial oxygen atoms from four distinct isonicotinate ligands and U−O bond lengths in the range 2.303(7) to 2.510(9) Å. The U≡O bond lengths are 1.735(10) and 1.767(10) Å, respectively. Each binuclear uranyl cluster is connected to another four Cu(I) cations through six isonicotinate anions, resulting in the final complicated three-dimensional coordination structure of **2** (Figure 2b). The bond-valence sums[57] of the U(VI) and Cu(I) centers in **2** are 6.1 and 1.2 vu, respectively, consistent with their formal valences and the typical red color of Cu(I).

In reported heterometallic UOFs with transition metals and carboxylate ligands the uranyl centers are linked to carboxylate groups, whereas the transition metals exhibit various coordination modes. Trinuclear uranyl motifs are relatively rare in UOFs, with only a few crystal structures documented.[2,58−62] Compound **1** appears to be the first example of a heterometallic UOF that contains trinuclear uranyl units. The U≡O and Cu− O bond distances are comparable to those reported that exhibit similar $U^{VI}{\equiv}O{-}Cu^{II}$ interactions.[9,11,34,50,51,63] In comparison with known Cu(II) heterometallic UOFs, the U≡O−Cu interaction and U−O−C−O−Cu bridging modes lead to a high dimensionality in **1**. For compound **2**, the absence of a U≡O− Cu interaction does not prevent the formation of a three-dimensional coordination network due to ligation saturation of the isonicotinate anions. The coordination modes of these anionic ligands are dissimilar to those recently reported for a uranylpyridinecarboxylate with Cu^{II} ions synthesized by either

using $Cu(NO_3)_2$ or copper metal as the transition metal source.[9,11,35,37,38] Notably, although quite a few copper−uranyl heterometallic UOFs have been reported, complex **2** contains monovalent Cu ions, which arise from in situ reduction of divalent Cu ions. The formation mechanism is assumed to be oxidation of chloride ions at low pH (ca. 3.04).

The EPR spectrum of complex **1** measured at room temperature is presented in Figure 4. The signal has an
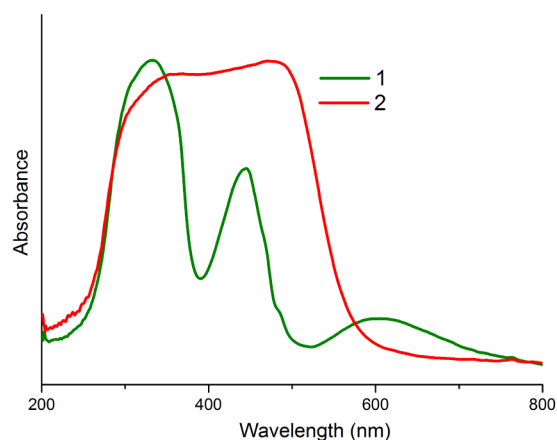

Figure 3. Absorption spectra for **1** and **2**.

anisotropic symmetry with $g_x = 2.2542$, $g_y = 2.0815$, $g_z = 2.0483$, and $A_x = 14.7$ mT. The EPR signal of complex **1** is typical for compounds containing copper(II) with d^9 electronic configuration. The symmetry of the registered signal is slightly rhombic, where the g value order $g_x \gg g_y > g_z > g_e$ ($g_e = 2.0023$) is characteristic for copper(II) in the $d(x^2-y^2)$ ground state.[64] The significant widening of the spectrum, especially of low-field components of hyperfine splitting, suggests strong interactions between copper and nitrogen atoms.[65]

Semi-quantitative EDS analyses indicate that elemental Cu:U ratios for compounds **1** and **2** are ∼1:3 and ∼1:1, in good agreement with the formulas provided by the single-crystal X-ray diffraction structure analyses. The Cu oxidation state of
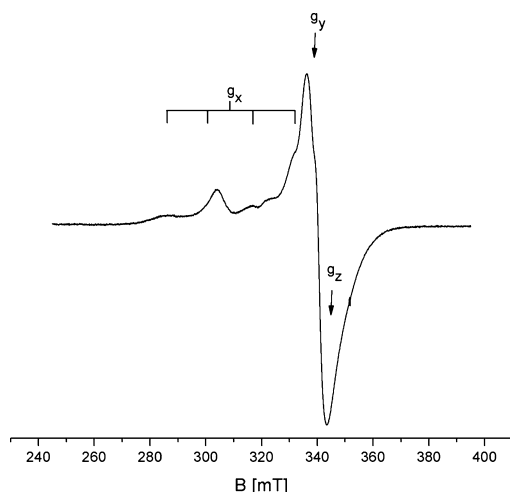
Figure 4. EPR spectrum of complex **1** at room temperature, microwave power 1 mW, modulation 1 G.

compound **2** was evaluated by X-ray photoelectron spectroscopy (XPS) at room temperature. The spectrum was fit using an iterated Shirley background and Gaussian-Lorentzian lineshape for the Cu $2p_{3/2}$ peak at 932.25 eV, as shown in Figure S3. The measured binding energy is comparable to corresponding values obtained for other Cu(I) compounds.[66,67]

The IR spectra (see Figure S4) of **1** and **2** both show strong bands at 909 cm^{-1} that arise from ν_3 $(UO_2)^{2+}$ stretching vibrations.[68] The Raman spectra (Figure S5) contain bands at 809 and 839 cm^{-1} for **1** and 840 and 865 cm^{-1} for **2** that are assigned to ν_1 $(UO_2)^{2+}$ symmetric stretching vibrations. On the basis of an empirical relationship for the uranyl ion bond length and the Raman frequency of the corresponding vibrations $[d(U-O)(pm) = 10650[\nu_1 \ (cm^{-1})]^{-2/3} + 57.5]$,[69] the predicted bond distances in **1** of 1.80 and 1.77 Å and in **2** of 1.77 and 1.75 Å are consistent with those from the structure analyses. The absorption spectra of both compounds show the typical $(UO_2)^{2+}$ bands at around 446 nm for **1** and 476 nm for **2**. The position of this transition varies compared with the typical vibrational-coupled electronic transition around 420 nm due to the chemical coordination environments about the U(VI) cations.[4,70] An additional absorbance peak in the spectrum of **1** at 608 nm is attributed to the d−d transition of the Cu(II) centers, as shown in Figure 3, and no such band was observed for compound **2**.

CONCLUSIONS

Reaction of uranyl acetate with either Cu(II) acetate or Cu(II) chloride in the presence of isonicotinic acid results in two three-dimensional frameworks of copper−uranium heterometallic compounds. Compound **1** presents an unusual interaction between the 5f U(VI) and 3d Cu(II) centers, and **2** exhibits the first example of a uranyl organic framework that includes a monovalent copper center. Presently, efforts are under way to define the mechanism of the reduction of copper in the formation of compound **2**.

ASSOCIATED CONTENT

S **Supporting Information**

Powder X-ray diffraction patterns, XPS spectrum of compound **2**, IR and Raman spectra, as well as crystallographic data of both heterometallic complexes (CIF). This material is available free of charge via the Internet at http://pubs.acs.org.

AUTHOR INFORMATION

Corresponding Author
*E-mail: pburns@nd.edu.

Notes
The authors declare no competing financial interest.

ACKNOWLEDGMENTS

REFERENCES

(1) Wang, K.-X.; Chen, J.-S. *Acc. Chem. Res.* **2011**, *44*, 531−540.
(2) Jiang, Y.-S.; Yu, Z.-T.; Liao, Z.-L.; Li, G.-H.; Chen, J.-S. *Polyhedron* **2006**, *25*, 1359−1366.
(3) Yu, Z.-T.; Liao, Z.-L.; Jiang, Y.-S.; Li, G.-H.; Chen, J.-S. *Chem.—Eur. J.* **2005**, *11*, 2642−2650.
(4) Weng, Z.; Wang, S.; Ling, J.; Morrison, J. M.; Burns, P. C. *Inorg. Chem.* **2012**, *51*, 7185−7191.
(5) Burns, P. C.; Ewing, R. C.; Hawthorne, F. C. *Can. Mineral.* **1997**, *35*, 1551−1570.
(6) Burns, P. C. *Can. Mineral.* **2005**, *43*, 1839−1894.
(7) Burns, P. C.; Ikeda, Y.; Czerwinski, K. *MRS Bull.* **2010**, *35*, 868−876.
(8) King, R. B. *Chem. Mater.* **2002**, *14*, 3628−3635.
(9) Olchowka, J.; Falaise, C.; Volkringer, C.; Henry, N.; Loiseau, T. *Chem.—Eur. J.* **2013**, *19*, 2012−2022.
(10) Andrews, M. B.; Cahill, C. L. *Chem. Rev.* **2013**, *113*, 1121−1136.
(11) Cahill, C. L.; de Lill, D. T.; Frisch, M. *CrystEngComm* **2007**, *9*, 15−26.
(12) Yang, W.; Dang, S.; Wang, H.; Tian, T.; Pan, Q.-J.; Sun, Z.-M. *Inorg. Chem.* **2013**, *52*, 12394−12402.
(13) Falaise, C.; Volkringer, C.; Vigier, J.-F.; Henry, N.; Beaurain, A.; Loiseau, T. *Chem.—Eur. J.* **2013**, *19*, 5324−5331.
(14) Cantos, P. M.; Jouffret, L. J.; Wilson, R. E.; Burns, P. C.; Cahill, C. L. *Inorg. Chem.* **2013**, *52*, 9487−9495.
(15) Thuéry, P. *Eur. J. Inorg. Chem.* **2013**, *2013*, 4563−4573.
(16) Thuéry, P. *Inorg. Chem.* **2013**, *52*, 435−447.
(17) Wang, C.-M.; Lii, K.-H. *J. Solid State Chem.* **2013**, *197*, 456−459.
(18) Adelani, P. O.; Oliver, A. G.; Albrecht-Schmitt, T. E. *Inorg. Chem.* **2012**, *51*, 4885−4887.
(19) Yu, Y.; Zhan, W.; Albrecht-Schmitt, T. E. *Inorg. Chem.* **2007**, *46*, 10214−10220.
(20) Tian, T.; Yang, W.; Pan, Q.-J.; Sun, Z.-M. *Inorg. Chem.* **2012**, *51*, 11150−11154.
(21) Alsobrook, A. N.; Zhan, W.; Albrecht-Schmitt, T. E. *Inorg. Chem.* **2008**, *47*, 5177−5183.
(22) Alsobrook, A. N.; Hauser, B. G.; Hupp, J. T.; Alekseev, E. V.; Depmeier, W.; Albrecht-Schmitt, T. E. *Cryst. Growth Des.* **2011**, *11*, 1385−1393.
(23) Alsobrook, A. N.; Hauser, B. G.; Hupp, J. T.; Alekseev, E. V.; Depmeier, W.; Albrecht-Schmitt, T. E. *Chem. Commun.* **2010**, *46*, 9167−9169.
(24) Alsobrook, A. N.; Alekseev, E. V.; Depmeier, W.; Albrecht-Schmitt, T. E. *Cryst. Growth Des.* **2011**, *11*, 2358−2367.
(25) Roy, S.; Mitra, P.; Patra, A. K. *Inorg. Chim. Acta* **2011**, *370*, 247−253.
(26) Weng, Z.; Chen, Z.; Qin, S.; Liang, F. *Inorg. Chim. Acta* **2009**, *362*, 3624−3628.

(27) Merkx, M.; Kopp, D. A.; Sazinsky, M. H.; Blazyk, J. L.; Müller, J.; Lippard, S. J. *Angew. Chem., Int. Ed.* **2001**, *40*, 2782−2807.

(28) Ferguson-Miller, S.; Babcock, G. T. *Chem. Rev.* **1996**, *96*, 2889−2908.

(29) Iwata, S.; Ostermeier, C.; Ludwig, B.; Michel, H. *Nature* **1995**, *376*, 660−669.

(30) Graziani, R.; Vidali, M.; Casellato, U.; Vigato, P. *Transition Met. Chem.* **1978**, *3*, 239−242.

(31) Salmon, L.; Thuéry, P.; Ephritikhine, M. *Polyhedron* **2007**, *26*, 631−636.

(32) Salmon, L.; Thuéry, P.; Ephritikhine, M. *Polyhedron* **2007**, *26*, 645−652.

(33) Salmon, L.; Thuery, P.; Riviere, E.; Girerd, J.-J.; Ephritikhine, M. *Chem. Commun.* **2003**, 762−763.

(34) Thuéry, P. *Inorg. Chem. Commun.* **2009**, *12*, 800−803.

(35) Frisch, M.; Cahill, C. L. *Dalton Trans.* **2005**, 1518−1523.

(36) Adelani, P. O.; Albrecht-Schmitt, T. E. *Cryst. Growth Des.* **2011**, *11*, 4676−4683.

(37) Frisch, M.; Cahill, C. L. *Dalton Trans.* **2006**, 4679−4690.

(38) Thuery, P.; Riviere, E. *Dalton Trans.* **2013**, *42*, 10551−10558.

(39) Stemmler, A. J.; Kampf, J. W.; Pecoraro, V. L. *Angew. Chem., Int. Ed. Engl.* **1996**, *35*, 2841−2843.

(40) Salmon, L.; Thuery, P.; Riviere, E.; Girerd, J.-J.; Ephritikhine, M. *Dalton Trans.* **2003**, 2872−2880.

(41) Salmon, L.; Thuéry, P.; Ephritikhine, M. *Polyhedron* **2003**, *22*, 2683−2688.

(42) Yu, Y.; Jiang, K.; Albrecht-Schmitt, T. E. *J. Solid State Chem.* **2009**, *182*, 1867−1871.

(43) Arnold, P. L.; Patel, D.; Blake, A. J.; Wilson, C.; Love, J. B. *J. Am. Chem. Soc.* **2006**, *128*, 9610−9611.

(44) Arnold, P. L.; Patel, D.; Wilson, C.; Love, J. B. *Nature* **2008**, *451*, 315−317.

(45) Locock, A. J.; Burns, P. C. *Can. Mineral.* **2003**, *41*, 489−502.

(46) Siegel, S.; Hoekstra, H. R. *Acta Crystallogr., Sect. B* **1968**, *24*, 967−970.

(47) Legros, J. P.; Jeannin, Y. *Acta Crystallogr., Sect. B* **1975**, *31*, 1133−1139.

(48) Shvareva, T. Y.; Albrecht-Schmitt, T. E. *Inorg. Chem.* **2006**, *45*, 1900−1902.

(49) Chen, W.; Yuan, H.-M.; Wang, J.-Y.; Liu, Z.-Y.; Xu, J.-J.; Yang, M.; Chen, J.-S. *J. Am. Chem. Soc.* **2003**, *125*, 9266−9267.

(50) Arnold, P. L.; Hollis, E.; White, F. J.; Magnani, N.; Caciuffo, R.; Love, J. B. *Angew. Chem., Int. Ed.* **2011**, *50*, 887−890.

(51) Volkringer, C.; Henry, N.; Grandjean, S.; Loiseau, T. *J. Am. Chem. Soc.* **2012**, *134*, 1275−1283.

(52) *APEXII*; Bruker AXS Inc.: Madison, WI, USA, 2007.

(53) Sheldrick, G. M. *SADABS-Bruker AXS Area Detector Scaling and Adsorption*; University of Gottingen: Germany, 2008.

(54) Sheldrick, G. M. *Acta Crystallogr., Sect. A* **2008**, *64*, 112−122.

(55) Macrae, C. F.; Bruno, I. J.; Chisholm, J. A.; Edgington, P. R.; McCabe, P.; Pidcock, E.; Rodriguez-Monge, L.; Taylor, R.; van de Streek, J.; Wood, P. A. *J. Appl. Crystallogr.* **2008**, *41*, 466−470.

(56) Liu, W.; Thorp, H. H. *Inorg. Chem.* **1993**, *32*, 4102−4105.

(57) Brese, N. E.; O'Keeffe, M. *Acta Crystallogr., Sect. B* **1991**, *47*, 192−197.

(58) Mihalcea, I.; Henry, N.; Volkringer, C.; Loiseau, T. *Cryst. Growth Des.* **2012**, *12*, 526−535.

(59) Lintvedt, R. L.; Heeg, M. J.; Ahmad, N.; Glick, M. D. *Inorg. Chem.* **1982**, *21*, 2350−2356.

(60) Thuéry, P. *Cryst. Growth Des.* **2011**, *11*, 2606−2620.

(61) Thuéry, P. *Cryst. Growth Des.* **2011**, *11*, 3282−3294.

(62) Szabó, Z.; Furó, I.; Csöregh, I. *J. Am. Chem. Soc.* **2005**, *127*, 15236−15247.

(63) Fortier, S.; Hayton, T. W. *Coord. Chem. Rev.* **2010**, *254*, 197−214.

(64) Garribba, E.; Micera, G. *J. Chem. Educ.* **2006**, *83*, 1229−1232.

(65) Mothilal, K. K.; Karunakaran, C.; Rao, P. S.; Murugesan, R. *Spectrochim. Acta, Part A* **2003**, *59*, 3337−3345.

(66) Uemura, K.; Ebihara, M. *Inorg. Chem.* **2013**, *52*, 5535−5550.

(67) Akitsu, T.; Einaga, Y. *Inorg. Chim. Acta* **2007**, *360*, 497−505.

(68) Bullock, J. I. *J. Inorg. Nucl. Chem.* **1967**, *29*, 2257−2264.

(69) Bartlett, J. R.; Cooney, R. P. *J. Mol. Struct.* **1989**, *193*, 295−300.

(70) Meinrath, G. *J. Radioanal. Nucl. Chem.* **1997**, *224*, 119−126.